

From Mono- and Dinuclear to Polynuclear Cobalt(II) and Cobalt(III) Coordination Compounds Based on *o*-Phthalic Acid and 2,2'-Bipyridine: Synthesis, Crystal Structures, and Properties

Svetlana G. Baca,^{*,[a]} Irina G. Filippova,^[b] Christina Ambrus,^[c] Maria Gdaniec,^[d] Yurii A. Simonov,^[b] Nicolae Gerbeleu,^[a] Olese A. Gherco,^[b] and Silvio Decurtins^[c]

Keywords: Carboxylate ligands / Cobalt / Magnetic properties / N ligands

The reaction of *o*-phthalic acid (H_2Pht) and 2,2'-bipyridine (bpy) with cobalt(II) carbonate at different temperatures results in the isolation of three types of new cobalt(II) and cobalt(III) compounds. The mononuclear cobalt(III) complex $[\text{Co}(\text{CO}_3)(\text{bpy})_2]_2(\text{Pht}) \cdot 16\text{H}_2\text{O}$ (**1**) is obtained when the reaction is run at 60 °C. Crystallographic analysis revealed that **1** contains two crystallographically independent $[\text{Co}(\text{CO}_3)(\text{bpy})_2]^+$ cations, a Pht^{2-} anion, and sixteen solvate water molecules. The latter form a wall of channels with the oxygen atoms of the carboxylate groups of the Pht^{2-} anions, which are occupied by pairs of cations. Increasing the temperature of the reaction to 80 °C leads to the formation of the open dinuclear cobalt(II) complex $[(\text{bpy})_2\text{Co}(\text{Pht})\text{H}(\text{Pht})\text{Co}(\text{bpy})_2] \cdot (\text{HPht})(\text{H}_2\text{Pht}) \cdot 2\text{H}_2\text{O}$ (**2**), which crystallizes in two polymorphic modifications **2a** and **2b**. Compound **2a** consists of a centrosymmetric dinuclear $[(\text{bpy})_2\text{Co}(\text{Pht})\text{H}(\text{Pht})\text{Co}(\text{bpy})_2]^+$ cation, an HPht^- anion, an H_2Pht molecule, and two solvate H_2O molecules. In **2b**, a small alteration in the crystal structure leads to an increase of the unit-cell volume. The asymmetric

unit of **2b** contains six crystallographically independent Co^{II} complexes, which combine into four $[(\text{bpy})_2\text{Co}(\text{Pht})\text{H}(\text{Pht})\text{Co}(\text{bpy})_2]^+$ units. The main structural unit of the cyclic dinuclear complex $[\text{Co}(\text{Pht})(\text{bpy})(\text{H}_2\text{O})]_2 \cdot 2\text{H}_2\text{O}$ (**4**) is neutral and centrosymmetric, with the two Co^{II} atoms linked by two phthalate ligands to form a 14-membered cycle. A further temperature increase results in the isolation of both the mononuclear complex $[\text{Co}(\text{Pht})(\text{bpy})(\text{H}_2\text{O})_3] \cdot 3\text{H}_2\text{O}$ (**3**) and the polynuclear helical coordination polymer $[\text{Co}(\text{Pht})(\text{bpy})(\text{H}_2\text{O})]_n$ (**5**). Extended hydrogen bonding networks as well as aromatic π - π stacking interactions stabilize multidimensional supramolecular architectures in all compounds. Magnetic susceptibility measurements have been performed for complexes **1**, **2**, **3**, and **5**. Simulations gave the following parameter sets: for complex **2** $|D| = 70 \text{ cm}^{-1}$, $g = 2.55$ and $J = -0.1 \text{ cm}^{-1}$; for complex **3** $|D| = 80 \text{ cm}^{-1}$, $g = 2.6$, and for complex **5** $|D| = 65 \text{ cm}^{-1}$, $g = 2.45$. Complex **1** is diamagnetic. © Wiley-VCH Verlag GmbH & Co. KGaA, 69451 Weinheim, Germany, 2005)

Introduction

Carboxylate complexes have received a great deal of attention over the last few years due to their interesting coordination chemistry, unusual structural features, remarkable physical and chemical properties, and extensive practical applications as dyes, extractants, drugs, pesticides, magnetic devices, etc.^[1] Metal carboxylates with a high stability are also efficient catalysts in a vast range of chemical and biochemical processes.^[2] Although a great number of metal carboxylates have been obtained to date, the rational design

and synthesis of novel metal carboxylates by employing new synthetic tools or by varying the nature of the reactants and synthetic conditions are currently under active investigation. In this context, *o*-phthalic acid (H_2Pht), which can exhibit a variety of coordination abilities^[3] and has a tendency to form large metal cluster aggregates^[4–9] or architectures with multi-dimensional frameworks, has been extensively explored. We have recently reported a series of nickel(II), copper(II), and zinc(II) phthalate compounds^[3,10–16] that show a great structural diversity, ranging from monomeric to polymeric assemblies. Herein we extend these studies to investigate the interactions of this universal ligand with cobalt ions in the presence of aromatic amines. In this respect, several cobalt phthalate compounds that are already known should be mentioned here. A very interesting example of a three-dimensional cobalt(II) polymer, namely $[\text{Co}(\text{Pht})_2(\text{bipy})]_n$ (bipy = 4,4'-bipyridine), which consists of interlinked Co–Pht–Co and Co–bpy–Co linear chains, has been reported by Lightfoot et al.^[17] Several dimers linked by *o*-phthalate $[\text{Co}_2(\text{Pht})(\text{L})(\text{H}_2\text{O})](\text{ClO}_4)_2$ (L = 2,2'-bipyridine, 1,10-phenanthroline, and 5-ni-

[a] Institute of Chemistry, Academy of Sciences of Moldova, Academiei 3 str., 2028 Chisinau, R. Moldova
Fax: +373-22-739611
E-mail: sbaca_md@yahoo.com

[b] Institute of Applied Physics, Academy of Sciences of Moldova, Academiei 5 str., 2028 Chisinau, R. Moldova

[c] Department of Chemistry and Biochemistry, University of Berne, 3012 Berne, Switzerland

[d] Faculty of Chemistry, A. Mickiewicz University, 60-780 Poznan, Poland

Supporting information for this article is available on the WWW under <http://www.eurjic.org> or from the author.

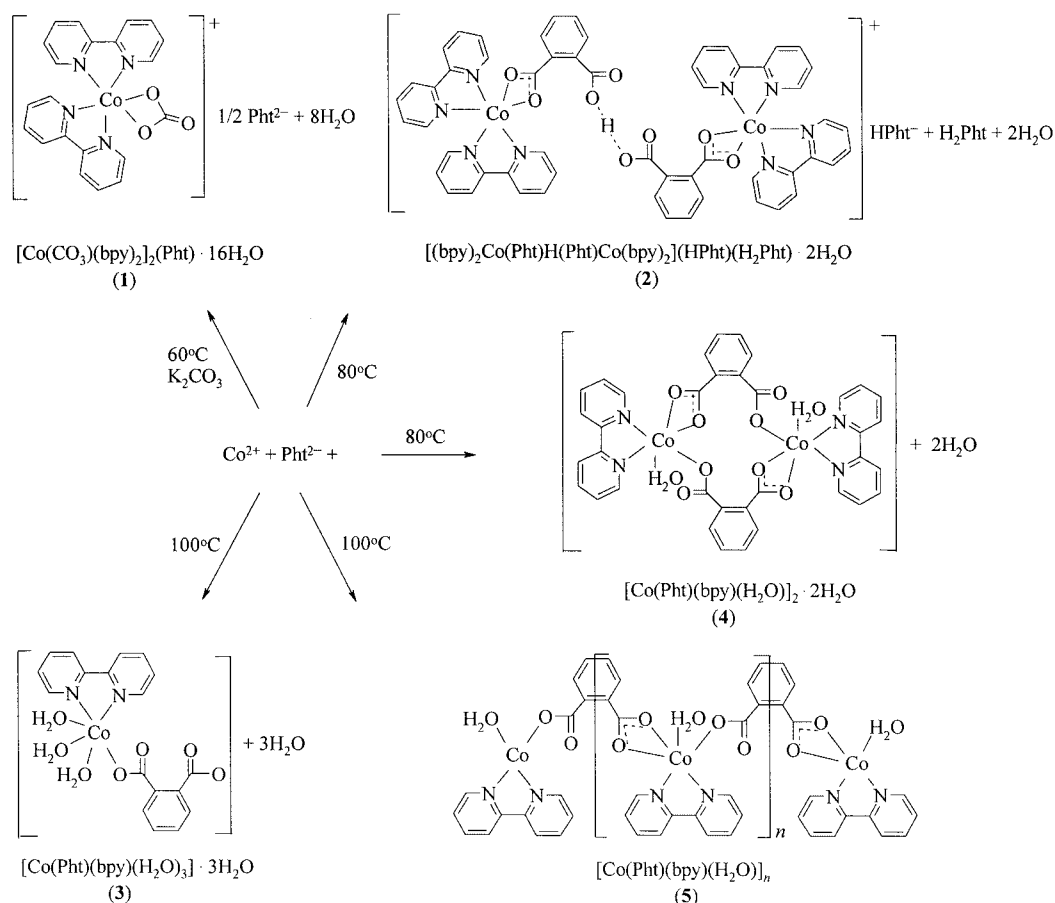
tro-1,10-phenanthroline) have also been isolated.^[18] Finally, the monomeric complexes $[\text{Co}(\text{Pht})(\text{phen})(\text{H}_2\text{O})_3] \cdot \text{H}_2\text{O}$ and $[\text{Co}(\text{Pht})(\text{dipy})] \cdot \text{H}_2\text{O}$ (phen = 1,10-phenanthroline, dipy = 2,2'-dipyridylamine) have been synthesized.^[19] Recently, we have also described the synthesis and structural characterization of cobalt(II) phthalate coordination polymers with derivatives of imidazole, for example 1-methylimidazole (1-MeIm),^[3] 2-methylimidazole (2-MeIm),^[12] and 4-methylimidazole (4-MeIm).^[15] In this paper we report on the synthesis, characterization, and crystal structures of three types of new cobalt(II) and cobalt(III) compounds with *o*-phthalic acid and 2,2'-bipyridine (bpy), namely the mononuclear cobalt(III) and cobalt(II) complexes $[\text{Co}(\text{CO}_3)(\text{bpy})_2]_2(\text{Pht}) \cdot 16\text{H}_2\text{O}$ (**1**) and $[\text{Co}(\text{Pht})(\text{bpy})(\text{H}_2\text{O})_3] \cdot 3\text{H}_2\text{O}$ (**3**), respectively, the open dinuclear complex $[(\text{bpy})_2\text{Co}(\text{Pht})\text{H}(\text{Pht})\text{Co}(\text{bpy})_2](\text{HPht})(\text{H}_2\text{Pht}) \cdot 2\text{H}_2\text{O}$ (**2**) and the cyclic dinuclear complex $[\text{Co}(\text{Pht})(\text{bpy})(\text{H}_2\text{O})]_2 \cdot 2\text{H}_2\text{O}$ (**4**), as well as the polynuclear helical coordination polymer $[\text{Co}(\text{Pht})(\text{bpy})(\text{H}_2\text{O})]_n$ (**5**).

Results and Discussion

Synthesis

The reaction of *o*-phthalic acid with cobalt(II) carbonate in the presence of amine at different temperatures affords

four new coordination compounds, as shown in Scheme 1. An oxidation of cobalt(II) ions to cobalt(III) was observed when the reaction was carried out at 60 °C in the presence of the base K_2CO_3 , and the reaction mixture was left in contact with air. This resulted in the formation of crystals of the cobalt(III) complex $[\text{Co}(\text{CO}_3)(\text{bpy})_2]_2(\text{Pht}) \cdot 16\text{H}_2\text{O}$ (**1**) in two weeks. To the best of our knowledge, **1** is the first example of a trivalent cobalt compound with *o*-phthalic acid, although in **1** the phthalate dianion is acting only as a counterion. It is interesting to note that similar bis(bipyridine)(carbonato)cobalt(III) nitrate and iodide complexes have also been obtained from the initial cobalt(II) salts but only under O_2 or CO_2 .^[20] It seems that the presence of aromatic amines such as bpy or phen facilitates the oxidation of the initial cobalt(II) species. Increasing the temperature of the reaction to 80 °C leads to the formation of the dimeric complex $[(\text{bpy})_2\text{Co}(\text{Pht})\text{H}(\text{Pht})\text{Co}(\text{bpy})_2](\text{HPht})(\text{H}_2\text{Pht}) \cdot 2\text{H}_2\text{O}$ (**2**), the identity of which was confirmed by X-ray crystallography. The two $[\text{Co}(\text{bpy})_2]^{2+}$ units in **2** are connected by a symmetric $\text{O} \cdots \text{H} \cdots \text{O}$ hydrogen bond between the carboxylate groups of two different coordinated phthalate ligands. A similar Zn compound has recently been reported.^[14] Compound **2** crystallizes from hot H_2O solution in two polymorphic modifications (**2a** and **2b**), which consist of similar structural units and differ in the crystal structure organization. Further increasing the reaction tempera-



Scheme 1.

ture resulted in the isolation of two new products, namely the coordination polymer $[\text{Co}(\text{Pht})(\text{bpy})(\text{H}_2\text{O})]_n$ (**5**) and the mononuclear complex $[\text{Co}(\text{Pht})(\text{bpy})(\text{H}_2\text{O})_3] \cdot 3\text{H}_2\text{O}$ (**3**), which were obtained in around 20% and 12% yields, respectively. One needs to mention here that the cyclic dimer **4** (Scheme 1) was obtained from the reaction of cobalt(II) acetate with H_2Pht and bpy in MeOH in a very low yield, therefore the sample was only suitable for X-ray studies. All attempts to optimize the yield of **4** were unsuccessful.

Spectroscopic Studies

The most relevant features of the IR spectra of compounds **1–3** and **5** are the absorptions due to the stretching of the dicarboxylate groups. The positions of these bands and the separations ($\Delta\nu$) between $\nu_{\text{asym}}(\text{CO}_2)$ and $\nu_{\text{sym}}(\text{CO}_2)$ indicate that the phthalate carboxylate groups function in different coordination modes. For complex **1**, in which the *o*-phthalic acid is fully deprotonated but acts only as a counterion, the characteristic bands of the uncoordinated carboxylate groups of Pht^{2-} appear at 1678 and 1564 cm^{-1} for asymmetric stretching, and at 1403 and 1382 cm^{-1} for symmetric stretching. In the IR spectrum of complex **2**, the medium-intensity peaks at 1717 and 1366 cm^{-1} also indicate the presence of uncoordinated *o*-phthalic acid [$\nu_{\text{asym}}(\text{CO}_2)$ for *o*-phthalic acid of 1690 and 1678 cm^{-1}].^[21] The absorptions at lower frequencies (1579 and 1411 cm^{-1}) can be attributed to deformation vibrations of the chelating carboxylate groups ($\Delta\nu = 168 \text{ cm}^{-1}$).^[22] The IR spectrum of **3** shows a broad $\nu_{\text{asym}}(\text{CO}_2)$ absorption with a maximum at 1568 cm^{-1} and a $\nu_{\text{sym}}(\text{CO}_2)$ absorption at 1404 cm^{-1} , which can be assigned to the chelating carboxylate group ($\Delta\nu = 164 \text{ cm}^{-1}$). For polymer **5**, the bands of the dicarboxylate groups appear at 1578 and 1543 cm^{-1} for the asymmetric stretching and at 1420 and 1385 cm^{-1} for the symmetric stretching. The $\Delta\nu$ values are 193 and 123 cm^{-1} and are attributed to the existence of both monodentate and chelating modes of the carboxylate groups, respectively. The infrared spectra of **1–3** and **5** also show broad bands in the 3634–3230 cm^{-1} region, which can be assigned to water molecules. Additionally, complex **1** has a strong band at 1638 cm^{-1} and a medium band at 1202 cm^{-1} , which are absent in the IR spectra of other complexes and are indicative of a chelating carbonate group.^[23]

Thermogravimetric Studies

Compounds **1–3**, and **5** were heated in the temperature range 25–600 °C. The TGA data show that the first weight loss corresponds to the removal of water molecules in all compounds. Complex **1** loses eleven water molecules in two steps from 30 to 150 °C (the total weight loss is 15.40%, calculated 15.07%). On further heating, **1** loses 43.88% of its weight between 160 and 270 °C, which corresponds to the release of the five remaining water molecules, the uncoordinated phthalate dianion (Pht^{2-}), and two bpy molecules

(calculated 43.08%). Complex **1** decomposes to the final product Co_2O_3 , with a remaining percentage of 13.22% (calculated 12.61%), when heated from 270 to 360 °C. For dimer **2**, the first weight loss is observed from 70 to 150 °C and is due to the loss of two water molecules (observed 2.51%, calculated 2.50%). In the temperature range of 170–510 °C the decomposition of the organic ligands takes place in four unidentified steps with a total weight loss of 85.91% to the final product CoO (found 11.39%, calculated 10.41%). For complex **3**, the first weight loss corresponding to both three uncoordinated and three coordinated water molecules (found 21.91%, calculated 22.17%) is found in the temperature range 30–150 °C. The second weight loss is observed from 150 to 320 °C and corresponds to the dissociation of the bpy ligand (found 30.31%, calculated 32.05%). The third weight loss of 19.58%, from 320 to 450 °C, is due to the loss of phenyl radical.^[24,25] A further weight loss of 11.49%, corresponding to the elimination of two molecules of CO ^[26] (calculated 12.15%), occurs between 450 and 540 °C. The final product is CoO , with a remaining percentage of 16.70% (calculated 15.37%). In contrast to **1–3**, the coordination polymer **5** is stable up to approximately 180 °C and then it loses 4.42% of its weight, which corresponds to the loss of a coordinated water molecule (calculated 4.53%). A further mass decrease is observed between 230 and 320 °C and corresponds to the loss of the bpy molecule (found 38.05%, calculated 39.32%). The decomposition of the Pht ligand is observed above 320 °C in two steps, with the weight loss of 18.65 and 14.10% each, by the removal of phenyl radical (calculated 20.28%) and two molecules of CO (calculated 15.93%), respectively, and is completed below 440 °C to give the expected oxide (found 20.15%, calculated 18.86%).

Description of the Crystal Structures

$[\text{Co}(\text{bpy})_2(\text{CO}_3)]_2(\text{Pht}) \cdot 16\text{H}_2\text{O}$ (**1**)

X-ray analysis indicates that the asymmetric unit of **1** contains two crystallographically independent $[\text{Co}(\text{CO}_3)(\text{bpy})_2]^+$ cations, a Pht^{2-} anion, and sixteen solvate water molecules (Figure 1). The structure of the cations is similar to that in the related compounds $[\text{Co}(\text{CO}_3)(\text{bpy})_2] \cdot \text{NO}_3 \cdot 5\text{H}_2\text{O}$ ^[20] and $[\text{Co}(\text{CO}_3)(\text{bpy})_2]\text{Cl} \cdot 3\text{H}_2\text{O}$.^[27] Each Co^{III} atom in **1** is coordinated by four nitrogen atoms of two chelating bpy molecules and two oxygen atoms of the chelating CO_3^- group, and thus adopts a distorted octahedral N_4O_2 environment. The average Co–N distances are 1.930 Å for $\text{Co}(1)$ and 1.932 Å for $\text{Co}(2)$, while the Co(1)–O bonds are 1.901(2) and 1.893(2) Å, with 1.895(2) and 1.898(2) Å for the Co(2)–O bonds (Table 1). The observed distortion from an octahedral geometry could be caused by the small bite angle of the chelating carbonate group [the O–Co–O angles are 69.42(8)° and 69.31(8)° for $\text{Co}(1)$ and $\text{Co}(2)$, respectively]. The O–Co–O bite angle of the chelating carbonate ligand agrees well with other bis(bipyridine)(carbonato)cobalt(III) [69.9(2)°]^[20] and (carbonato)bis(phenanthroline)cobalt(III) complexes [varies from 68.4(5)° to

69.8(2)°.^[20,28] The dihedral angles between the four-membered chelate ring of the carbonate group and two five-membered chelate rings of the bpy ligands are 94.6(1)° and 87.0(1)° for Co(1), and 87.0(1)° and 96.5(1)° for Co(2).

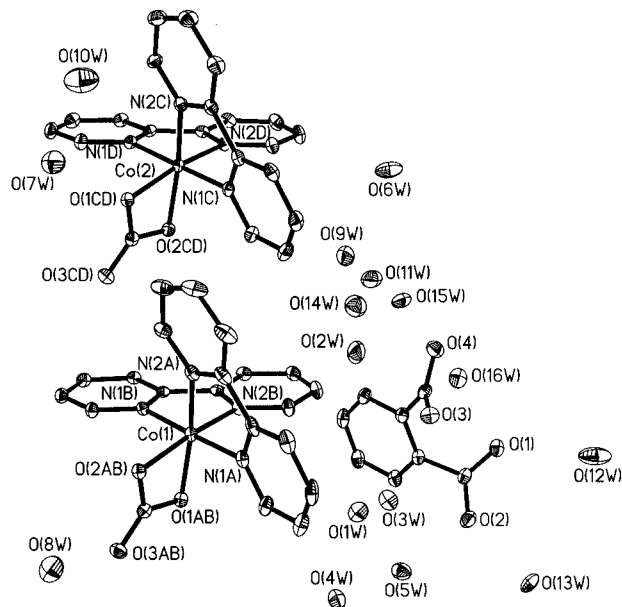


Figure 1. Crystallographically independent structure fragment with numbering scheme and displacement ellipsoids drawn at the 30% probability level in compound **1**. Two water molecules are disordered over two positions: O(13w) and O(13*), O(14w) and O(14*). Hydrogen atoms have been omitted for clarity.

Table 1. Selected bond lengths [Å] and angles [°] for compound **1**.

Co(1)–O(1AB)	1.901(2)	Co(2)–O(1CD)	1.895(2)
Co(1)–O(2AB)	1.893(2)	Co(2)–O(2CD)	1.898(2)
Co(1)–N(1A)	1.920(2)	Co(2)–N(1C)	1.922(2)
Co(1)–N(1B)	1.926(2)	Co(2)–N(1D)	1.934(2)
Co(1)–N(2A)	1.927(2)	Co(2)–N(2C)	1.933(2)
Co(1)–N(2B)	1.947(2)	Co(2)–N(2D)	1.937(2)
O(1AB)–Co(1)–O(2AB)	69.42(8)	O(1CD)–Co(2)–O(2CD)	69.31(8)
O(1AB)–Co(1)–N(1A)	92.76(9)	O(1CD)–Co(2)–N(1C)	89.20(9)
O(1AB)–Co(1)–N(1B)	88.65(9)	O(1CD)–Co(2)–N(1D)	91.59(9)
O(1AB)–Co(1)–N(2A)	165.96(8)	O(1CD)–Co(2)–N(2C)	97.66(9)
O(1AB)–Co(1)–N(2B)	99.21(9)	O(1CD)–Co(2)–N(2D)	165.43(8)
O(2AB)–Co(1)–N(1A)	88.91(8)	O(2CD)–Co(2)–N(1C)	92.41(9)
O(2AB)–Co(1)–N(1B)	92.53(8)	O(2CD)–Co(2)–N(1D)	87.95(9)
O(2AB)–Co(1)–N(2A)	96.95(9)	O(2CD)–Co(2)–N(2C)	166.34(9)
O(2AB)–Co(1)–N(2B)	167.92(9)	O(2CD)–Co(2)–N(2D)	96.85(9)
N(1A)–Co(1)–N(1B)	178.26(9)	N(1C)–Co(2)–N(1D)	179.21(9)
N(1A)–Co(1)–N(2B)	95.92(9)	N(1C)–Co(2)–N(2C)	83.04(9)
N(1A)–Co(1)–N(2A)	83.36(10)	N(1C)–Co(2)–N(2D)	96.13(9)
N(1B)–Co(1)–N(2A)	95.50(10)	N(2C)–Co(2)–N(1D)	96.77(10)
N(1B)–Co(1)–N(2B)	82.85(9)	N(1D)–Co(2)–N(2D)	83.13(9)
N(2A)–Co(1)–N(2B)	94.61(9)	N(2C)–Co(2)–N(2D)	96.44(9)

Pht²⁻ acts as a fully deprotonated counterion. The average dihedral angle between the planes of its carboxylate groups is 60.6°, and the angles between the planes of the carboxylate groups and the aromatic ring are 48.8° and 52.1°. The sixteen solvent water molecules and the uncoordinated oxygen atoms of the carboxylate groups of the Pht²⁻ anion form a system of hydrogen bonds that generate a wall of channels. These channels are extended along the *b* axis (Figure 2) and are occupied by pairs of [Co(CO₃)-

(bpy)₂]⁺ cations. The latter are attached to the channels' walls by hydrogen bonds [O(4w)–H···O(3CD) = 2.800(3), O(8w)–H···O(3AB) = 2.814(3), and O(7w)–H···O(1CD) = 2.811(3) Å], as well as by π – π interactions between the Pht ring and the pyridine ring from the Co(1) complex [the centroid–centroid distance is 3.562(2) Å].

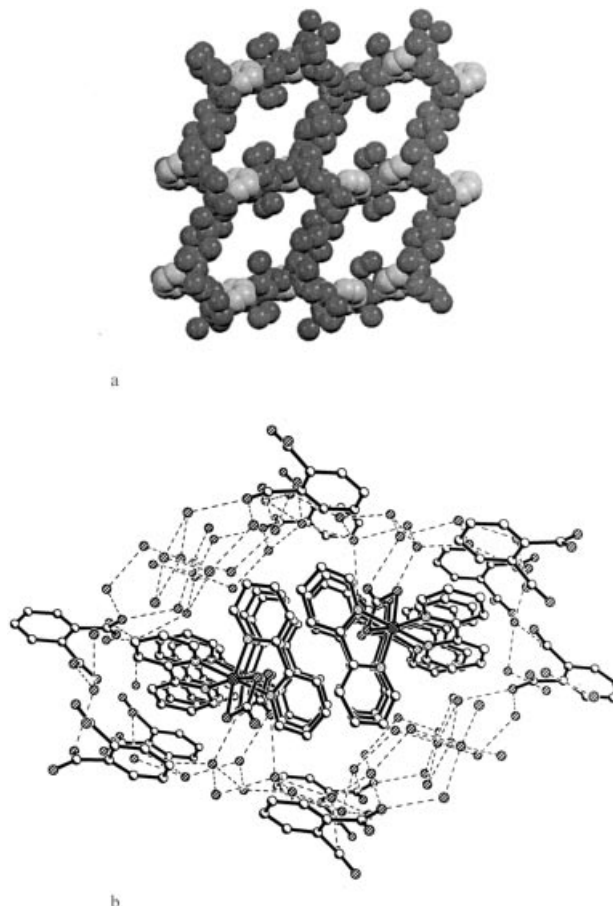


Figure 2. (a) Space-filling representation of channels in the structure of compound **1**. Cations [Co(bpy)₂(CO₃)]⁺ have been omitted for clarity. (b) One channel with a pair of columns formed by [Co(bpy)₂(CO₃)]⁺ cations in **1**. Hydrogen atoms have been omitted for clarity and hydrogen bonds are indicated by dotted lines.

The cations are arranged in pairs of columns due to π – π stacking interactions between the antiparallel aromatic rings belonging to two Co(1) complexes and related by a symmetrical center at the (1/2, 1/2, 0) site (Figure 2b). The average contact distance of the adjacent aromatic rings is about 3.52 Å and the centroid–centroid distance is 3.780(2) Å. The corresponding distances for analogous pyridine rings of two Co(2) complexes are about 3.77 and 3.987(1) Å, respectively, and are slightly longer than those for typical aromatic–aromatic π –stacking interactions.^[29] Weak C–H···O hydrogen bonds between the CH groups of the pyridine rings and the uncoordinated oxygen atoms of the CO₃ ligands join Co(1) and Co(2) complexes within the column [C(11C)–H···O(3AB) = 3.226 Å, C(11A)–H···O(3CD) = 3.215 Å].

[(bpy)₂Co(Pht)H(Pht)Co(bpy)₂](HPht)(H₂Pht)·2H₂O (2a, 2b)

X-ray diffraction analysis revealed that compound **2** crystallizes in two polymorphic forms: **2a** and **2b** (Table 2). The unit-cell parameters of **2a** and **2b** are related as follows: $a_{2b} \approx -(a_{2a} + c_{2a})$; $b_{2b} \approx b_{2a} + c_{2a} - a_{2a}$; $c_{2b} \approx 2(a_{2a} + b_{2a})$.

The former (**2a**) is isostructural with the analogous Zn complex^[14] and also consists of a centrosymmetric dinuclear $[(bpy)_2Co(Pht)H(Pht)Co(bpy)_2]^+$ cation, an HPht[−] anion, an H₂Pht molecule, as well as two solvate H₂O molecules (Figure 3). Each Co atom has a distorted octahedral geometry containing four nitrogen atoms of two bpy ligands (the average Co–N bond length is 2.107 Å) and two oxygen atoms from one chelating carboxylate group of the Pht ligand [Co–O 2.112(2) and 2.225(2) Å]. The angle of the chelating carboxylate group O(3)–Co(1)–O(4) is 60.85(6)°. This value is in good agreement with those of similar 3d-metal complexes with a 1,3-chelating bidentate function of the Pht ligand.^[10–15] It should be noted that the coordinated carboxylate group of the Pht residue in **2a** is almost coplanar with the aromatic ring – the dihedral angle between them is 10.2(1)°; for the second carboxyl group this angle is equal to 74.1(1)°. The two mononuclear structural units consisting of one metal ion, two bpy molecules, and one residue of *o*-phthalic acid are linked by a very short symmetric O···H···O hydrogen bond of 2.447(3) Å between the carboxylate oxygen atoms O(1) and O(1A) into a dimer. Consequently, the metal-containing backbone can be considered as a $[(bpy)_2Co(Pht)H(Pht)Co(bpy)_2]^+$ unit.

The dinuclear aggregate forms a hydrogen-bonded network with water molecules and the uncoordinated molecule of *o*-phthalic acid. The position of the hydrogen atoms of the carboxylic groups in the uncoordinated phthalate molecules could not be located because of disorder of oxygen atoms over two orientations with 50% probability. Therefore, we propose a model in which the crystal of **2a** contains

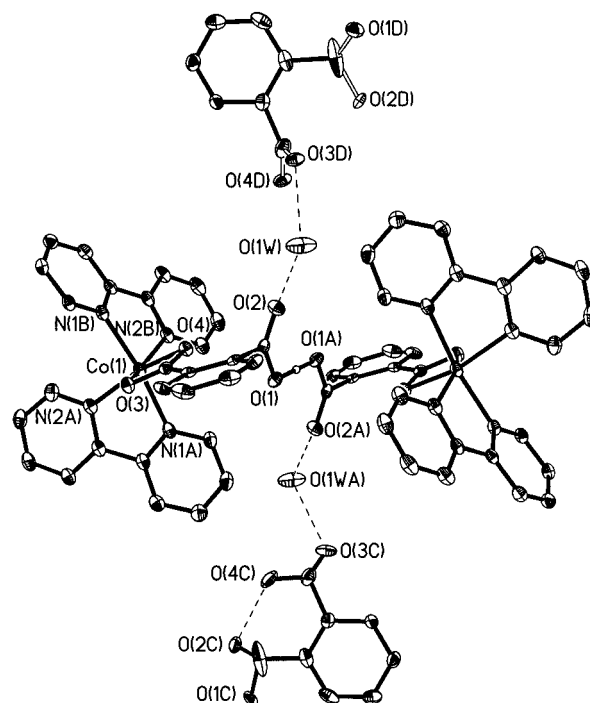


Figure 3. Dimeric aggregate in compound **2a**. Two configurations of the uncoordinated molecule of *o*-phthalic acid with C and D index are shown. All hydrogen atoms except a symmetric O(1)···H···O(1A) bond in the dimer have been omitted for clarity.

chains formed by an alternation of neutral H₂Pht molecules, water molecules, and monodeprotonated hydrogen phthalate anions (HPht[−]), as shown in Figure 4. In this case, the inversion centers between two disordered carboxylic groups of the neighboring uncoordinated phthalate moieties in the chains have a statistical character (Figure 4). Variations of analogous chains have been observed in $\{[(\eta^6-C_6H_6)_2Cr]^+[HPht][H_2Pht]\}$ as well as in $\{[(\eta^5-C_5H_5)_2-$

Table 2. Selected bond lengths [Å] and angles [°] of the two polymorphic forms of **2** (**2a** and **2b**).

2a		2b	Min value, max value	Average
Co(1)–O(3)	2.225(2)	Co–O(3)	2.213(2), 2.259(3)	2.233
Co(1)–O(4)	2.112(2)	Co–O(4)	2.099(2), 2.132(2)	2.116
Co(1)–N(1A)	2.119(2)	Co–N(1A)	2.105(3), 2.142(3)	2.121
Co(1)–N(1B)	2.105(1)	Co–N(1B)	2.096(3), 2.117(3)	2.106
Co(1)–N(2A)	2.119(2)	Co–N(2A)	2.108(3), 2.144(3)	2.127
Co(1)–N(2B)	2.086(2)	Co–N(2B)	2.088(3), 2.103(3)	2.095
O(4)–Co(1)–O(3)	60.85(6)	O(4)–Co–O(3)	60.0(1), 60.8(1)	60.4
N(1B)–Co(1)–O(4)	96.25(7)	O(4)–Co–N(1B)	96.4(1), 97.4(1)	96.5
N(2B)–Co(1)–O(4)	93.64(7)	N(2B)–Co–O(4)	93.5(1), 94.3(1)	93.9
N(1A)–Co(1)–O(3)	88.83(7)	N(1A)–Co–O(3)	88.1(1), 90.0(1)	89.1
O(4)–Co(1)–N(1A)	92.82(7)	O(4)–Co–N(1A)	92.4(1), 93.6(1)	93.0
N(1B)–Co(1)–N(1A)	170.88(7)	N(1B)–Co–N(1A)	170.0(1), 171.0(1)	170.5
N(2B)–Co(1)–N(1A)	102.29(8)	N(2B)–Co–N(1A)	100.8(1), 102.4(1)	101.7
N(1B)–Co(1)–O(3)	94.73(7)	N(1B)–Co–O(3)	95.0(1), 96.0(1)	95.6
N(2B)–Co(1)–N(1B)	78.14(8)	N(2B)–Co–N(1B)	77.2(1), 78.3(1)	77.7
N(2A)–Co(1)–O(3)	99.90(7)	N(2A)–Co–O(3)	98.5(1), 101.5(1)	100.1
O(4)–Co(1)–N(2A)	159.02(7)	O(4)–Co–N(2A)	157.2(1), 159.7(1)	158.6
N(1A)–Co(1)–N(2A)	77.61(8)	N(1A)–Co–N(2A)	76.7(1), 77.6(1)	77.1
N(1B)–Co(1)–N(2A)	93.49(8)	N(1B)–Co–N(2A)	93.0(1), 94.8(1)	93.9
N(2B)–Co(1)–N(2A)	106.55(8)	N(2B)–Co–N(2A)	105.2(1), 107.7(1)	106.6
N(2B)–Co(1)–O(3)	152.91(7)	N(2B)–Co–O(3)	152.1(1), 153.6(1)	152.8

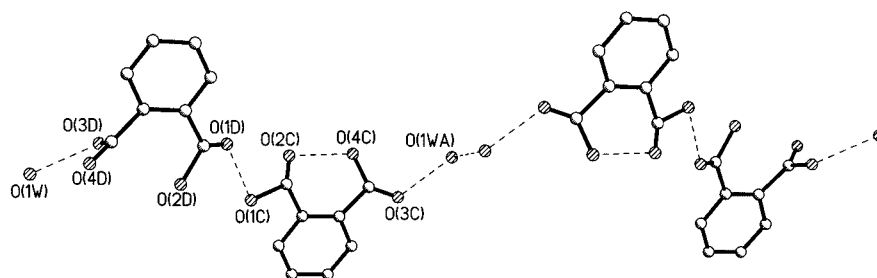


Figure 4. One version of a chain in **2a**. The molecule of Pht with D index is neutral and another one with C index is monodeprotonated.

$\text{Co}]^+)_4([\text{HPht}]^-)_2[\text{Pht}]^{2-}\}$.^[30] The neutral molecule of *o*-phthalic acid forms two hydrogen bonds: $\text{O}(1\text{D})\cdots\text{O}(1\text{C}) = 2.588(6) \text{ \AA}$ and $\text{O}(3\text{D})\cdots\text{O}(1\text{w}) = 2.582(6) \text{ \AA}$. Another conformer acts as a monoanion with only one short intramolecular hydrogen bond [$\text{O}(4\text{C})\cdots\text{O}(2\text{C}) = 2.390(6) \text{ \AA}$]. Two water molecules join pairs of H_2Pht – HPht^- units into zig-zag chains through $\text{O}–\text{H}\cdots\text{O}$ hydrogen bonds: $\text{O}(1\text{w})\cdots\text{O}(1\text{wA})$ ($-x + 1, -y + 2, -z$) = $2.690(4) \text{ \AA}$, or $\text{O}(1\text{w})\cdots\text{O}(3\text{C}) = 2.702(6) \text{ \AA}$. The dinuclear aggregates are attached on both sides of the chains due to hydrogen bonds [$\text{O}(1\text{w})–\text{H}\cdots\text{O}(2) = 2.795(3) \text{ \AA}$].

Other noncovalent forces that contribute significantly to the 3D structural organization of **2a** should be mentioned, namely aromatic π – π interactions between the uncoordinated phthalate moieties and one of the coordinated bpy molecules (with A indexes), with a centroid–centroid distance of 3.754 \AA . The angle between the overlapping aromatic system is $8.3(1)^\circ$. There are also π – π stacking interactions between the antiparallel bpy ligands from different dinuclear aggregates (the dihedral angle between the bpy planes being 0° , with a distance between the centroids of the bpy rings of 3.748 \AA for the A molecules of bpy and 3.697 \AA for B). The uncoordinated phthalate moieties also take part in a $\text{C}–\text{H}\cdots\pi$ interaction with the B bpy molecule [the distance between $\text{H}(5\text{C})$ and the centroid of the surrounding B ring is 2.646 \AA]. Weak $\text{C}–\text{H}\cdots\text{O}$ hydrogen bonds involving the bpy carbon atoms and both the coordinated

carboxylate oxygen atom (3.273 \AA) and the oxygen atoms of the uncoordinated phthalate molecules (3.059 and 3.275 \AA for two possible orientations) are also worthy of mention.

In compound **2b**, a small alteration in the crystal structure increases the unit cell's volume six times compared with that of **2a**. The asymmetric unit of **2b** contains six crystallographically independent Co^{II} complexes, which combine in the crystal structure into four $[(\text{bpy})_2\text{Co}(\text{Pht})\text{H}(\text{Pht})\text{Co}(\text{bpy})_2]^+$ units, as shown in Figure 5. Two of them, namely $\text{Co}(5)–\text{Co}(5\text{A})$ and $\text{Co}(6)–\text{Co}(6\text{A})$, are centrosymmetric, while the others [$\text{Co}(1)–\text{Co}(2)$ and $\text{Co}(3)–\text{Co}(4)$] are noncentrosymmetric. A comparison of the main bond lengths and angles in all six Co complexes shows a close similarity between them. The average structural parameters of the coordination environment of the Co atoms are listed in Table 2. The maximum dispersion of distances in Co distorted octahedrons was observed for the $\text{Co}–\text{O}(3)$ bond lengths, which are in the range $2.259(3)–2.213(2) \text{ \AA}$. The $\text{Co}–\text{O}(4)$ bond lengths vary from $2.099(2)$ to $2.132(3) \text{ \AA}$. In the case of $\text{Co}–\text{N}$ distances, their values are in the range $2.088(3)–2.144(3) \text{ \AA}$, but the interval of bond lengths for each bpy molecule is not more than 0.037 \AA .

The crystal structure of **2b** is organized in an analogous manner to **2a**. Every Co complex has satellite uncoordinated phthalate moieties connected to a bpy molecule by a π – π stacking interaction (the distance between the overlap-

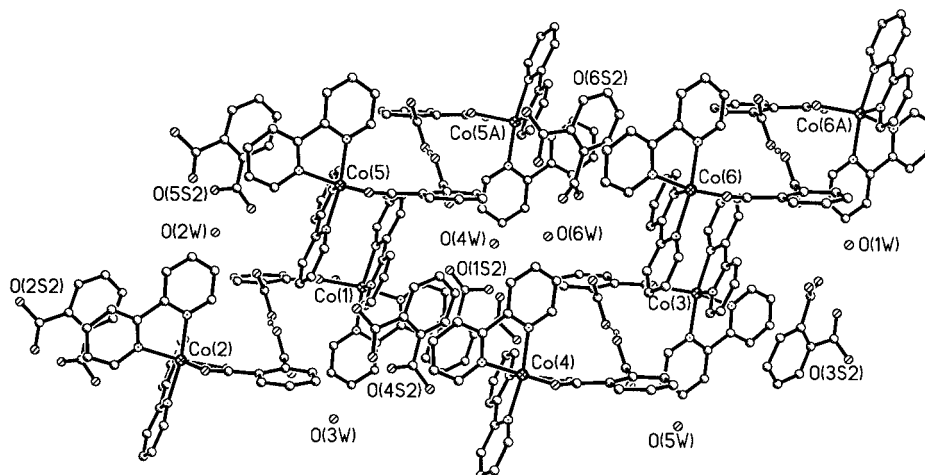


Figure 5. Six crystallographically independent Co complexes, which form four $[(\text{bpy})_2\text{Co}(\text{Pht})\text{H}(\text{Pht})\text{Co}(\text{bpy})_2]^+$ units in compound **2b**. Hydrogen atoms have been omitted for clarity.

ping aromatic rings is about 3.76 Å). Six Pht^{2-} anions compensate the charge of the dimeric units and take part in the formation of H-bonded chains that are similar to those in **2a** (Figure 4). There are four crystallographically independent chains in **2b**. The quality and volume of experimental data, as well as the disorder of some carboxylate groups of the Pht moieties and water molecules, did not permit the localization of all the hydrogen atoms in the structure. However, the possibility to distinguish both the neutral H_2Pht and monodeprotonated HPht^- anion exists for the four molecules. Molecules with indexes 1S and 5S are neutral H_2Pht , while 3S and 6S molecules are HPht^- anions, and the chains may be described as $-\text{O}(1\text{S})-\text{H}\cdots\text{O}(4\text{w})\{\text{or O}(4\text{w}')\}-\text{H}\cdots\text{O}(6\text{w})\{\text{or O}(6\text{w}')\}-\text{H}\cdots\text{O}(6\text{S})-$ and $-\text{O}(5\text{S})-\text{H}\cdots\text{O}(2\text{w})\{\text{or O}(2\text{w}')\}-\text{H}\cdots\text{O}(1\text{w})\{\text{or O}(1\text{w}')\}-\text{H}\cdots\text{O}(3\text{S})-$. The distribution of the carboxylic H atom for the two remaining disordered phthalate moieties (2S and 4S) has statistical character as in **2a**. The dinuclear aggregates are attached on both sides of the chains due to $\text{O}(\text{w})-\text{H}\cdots\text{O}_{\text{carb}}$ hydrogen bonds that are in the range 2.79(1)–2.98(1) Å. An additional $\pi-\pi$ interaction occurs between the bpy molecules of adjacent Co complexes: Co(3) and Co(6), Co(1) and Co(5), Co(2) and Co(4).

An analysis of the charges on the four different supramolecular aggregates consisting of a $[(\text{bpy})_2\text{Co}(\text{Pht})\text{H}(\text{Pht})\text{Co}(\text{bpy})_2]^+$ unit and two satellite uncoordinated phthalate moieties (monodeprotonated or neutral) shows that the structure of **2b** has four types of supramolecular fragments. Two of them are formed around the centrosymmetric dimers Co(5)–Co(5A) and Co(6)–Co(6A) and have a positive charge $\{(\text{H}_2\text{Pht})[(\text{bpy})_2\text{Co}(5)(\text{Pht})\text{H}(\text{Pht})\text{Co}(5\text{A})(\text{bpy})_2]-(\text{H}_2\text{Pht})\}^+$ and negative charge $\{(\text{HPht})[(\text{bpy})_2\text{Co}(6)(\text{Pht})\text{H}(\text{Pht})\text{Co}(6\text{A})(\text{bpy})_2](\text{HPht})\}^-$, respectively. The supramolecular aggregate around Co(1)–Co(2) is statistically neutral or has charge +1, and the one around Co(3)–Co(4) has a 0 or –1 charge. This effect could explain the increase of the cell volume in **2b**.

$[\text{Co}(\text{Pht})(\text{bpy})(\text{H}_2\text{O})_3]\cdot 3\text{H}_2\text{O}$ (**3**)

Compound **3** (Figure 6) may be subsumed to the structural type $[\text{M}(\text{Pht})(\text{Amin})(\text{H}_2\text{O})_3]\cdot n\text{H}_2\text{O}$ [$\text{M} = \text{Co}, \text{Ni}$; Amin = one bidentate ligand (bpy, dipya, phen)^[19,31] or two monodentate ligands (Py, β -Pic, 1-MeIm);^[32] $n = 0, 1, 3$]. In all these compounds, the *o*-phthalic acid residue is fully deprotonated and acts as a monodentate ligand. The Co atom in **3** is in a distorted octahedral environment, being coordinated by two nitrogen atoms from the bpy molecule, with a Co–N(1) distance of 2.126(1) Å and a Co–N(2) distance of 2.134(1) Å, the O(4) atom of the monocoordinated phthalate ligand [2.145(1) Å], and three oxygen atoms of water molecules [O(1w), O(2w), and O(3w) distances of 2.115(1), 2.112(1), and 2.056(1) Å, respectively] (Table 3). The water molecules O(1w) and O(2w) are *trans* to N(1) and N(2), respectively, whereas O(3w) lies *trans* to O(4). Thus, three coordinated water molecules make one edge of the octahedron, whereas the same coordinated water molecules lie in a meridian place in the related compounds.^[19,30,31] However, the main features of the crystal

packing in compound **3** are maintained. In all these compounds the coordinated and uncoordinated water molecules form both intramolecular and intermolecular hydrogen bonds leading to the organization of double-chains.^[32] The arrangement of these chains mainly depends on the nature of the aromatic amine. The presence of supplementary out-of-sphere water molecules in compound **3** generates a 3D network held together by $\text{O}-\text{H}\cdots\text{O}$ hydrogen bonds. The water molecule O(2w) and the carboxylate oxygen atom O(3) are involved in intramolecular H-bonding [O(2w)–H \cdots O(3) = 2.831(2) Å] forming a six-membered hydrogen-bonded Co(1)–O(2w)–H \cdots O(3)–C(22)–O(4)–Co(1) ring (Figure 6). Individual molecules are joined into centrosymmetric dimers by the hydrogen bonds O(2w)–H \cdots O(2) [2.678(2) Å] and O(3w)–H \cdots O(1) [2.713(2) Å] (symmetry code for O(2) and O(3): $-x + 1, -y + 1, -z$). The Co \cdots Co distance within the dimer is 7.368(1) Å. These dimeric units are further connected by $\text{O}(\text{w})-\text{H}\cdots\text{O}(\text{carb.})$ and $\text{O}(\text{w})-\text{H}\cdots\text{O}(\text{w})$ hydrogen bonds into double-chains running along the *a* axis of the unit cell of **3** (Figure 7). The distance between the metal centers of the adjacent dimers is 6.698(1) Å. The hydrogen bond O(4w)–H \cdots O(6w) ($x, -y + 1/2, z - 1/2$) of 2.775(2) Å and possible $\pi-\pi$ interactions between antiparallel molecules of bpy (the average distances

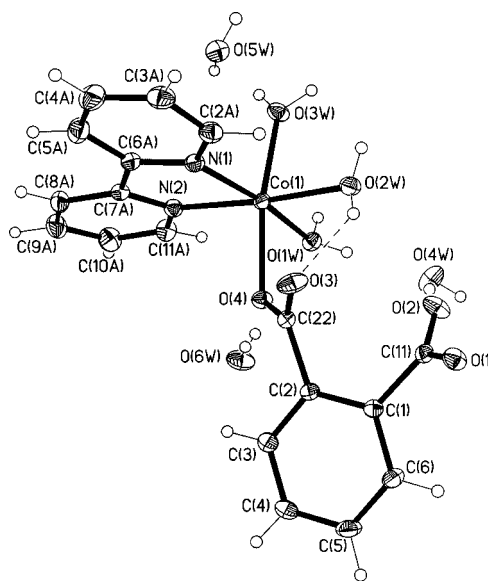


Figure 6. Molecular structure of compound **3**.

Table 3. Selected bond lengths [Å] and angles [°] for compound **3**.

Co(1)–O(4)	2.145(1)	Co(1)–O(1w)	2.115(1)
Co(1)–N(1)	2.126(1)	Co(1)–O(2w)	2.112(1)
Co(1)–N(2)	2.134(1)	Co(1)–O(3w)	2.056(1)
N(1)–Co(1)–O(4)	96.46(5)	O(2w)–Co(1)–O(4)	87.79(5)
N(1)–Co(1)–N(2)	77.36(5)	O(2w)–Co(1)–N(1)	97.29(5)
N(2)–Co(1)–O(4)	95.16(5)	O(2w)–Co(1)–N(2)	174.13(5)
O(3w)–Co(1)–O(4)	170.06(4)	O(2w)–Co(1)–O(3w)	91.17(5)
O(3w)–Co(1)–N(1)	91.36(5)	O(1w)–Co(1)–O(4)	81.87(5)
O(3w)–Co(1)–N(2)	92.53(5)	O(1w)–Co(1)–N(1)	171.32(5)
O(3w)–Co(1)–O(2w)	85.13(5)	O(1w)–Co(1)–N(2)	94.27(5)
O(3w)–Co(1)–O(1w)	91.29(5)		

between the overlapping rings are 3.56 and 3.23 Å) link the double chains into a 3D network (Figure 8).

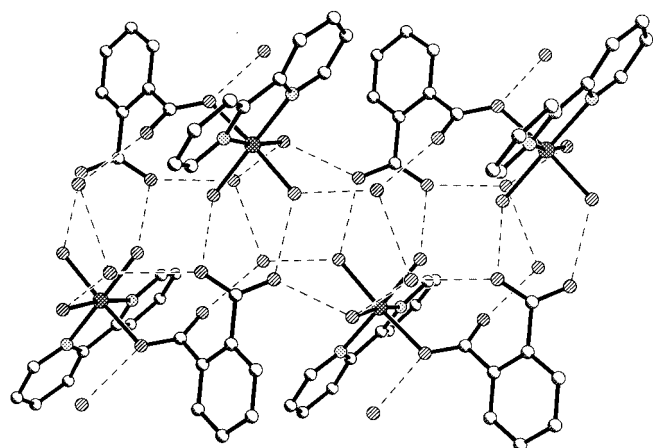


Figure 7. View of a double-chain in compound 3. Hydrogen atoms have been omitted for clarity and hydrogen bonds are indicated by dotted lines.

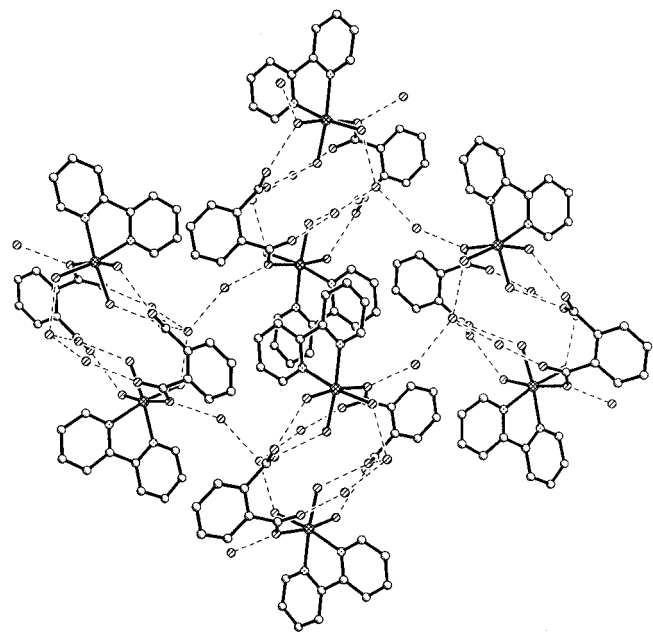


Figure 8. Packing diagram of compound 3. Hydrogen atoms have been omitted for clarity and hydrogen bonds are indicated by dotted lines.

$[\text{Co}(\text{Pht})(\text{bpy})(\text{H}_2\text{O})]_2 \cdot 2\text{H}_2\text{O}$ (4)

A neutral centrosymmetric dinuclear aggregate $[\text{Co}(\text{Pht})(\text{bpy})(\text{H}_2\text{O})]_2$ is the main structural unit of compound 4, in which two Co^{II} atoms are linked by two phthalate ligands to form a 14-membered cycle (Figure 9). The coordination modes of the two deprotonated carboxylate groups in the Pht residue are different. One carboxylate group is bidentate to a Co atom, while the other one is monocoordinated to the adjacent Co atom. The Co atoms are in a distorted octahedral environment. Deformation of the Co^{II} coordination polyhedron is observed both in bond lengths [range from 2.076(1) to 2.235(2) Å] and angles

$[\text{O}(3)-\text{Co}-\text{O}(4) = 60.15^\circ$; Table 4]. The Co atom is coordinated by three oxygen atoms $[\text{O}(1^*), \text{O}(3), \text{O}(4)]$ from two Pht residues [2.141(1), 2.235(2), and 2.076(1) Å], one water molecule $[\text{O}(1\text{w}) 2.118(1) \text{ Å}]$, and two nitrogen atoms $[\text{N}(1), \text{N}(2)]$ of a bpy molecule [2.097(1) and 2.127(1) Å]. The $\text{Co} \cdots \text{Co}$ distance in this dimer is 5.034(1) Å. Similar dimers have been described recently in $[\text{Zn}(\text{Pht})(\text{Im})(\text{H}_2\text{O})]_2$,^[13] although in this latter complex the Pht ligands exhibit a 1,6-bridging function and the Zn atoms have a tetrahedral environment. A 14-membered cycle is formed in both compounds, but alteration of the structural function of the Pht residue leads to a shorter transannular distance in 4 $[\text{O}(4)-\text{O}(4^*) = 3.448(2) \text{ Å}]$ compared to that in the Zn dimer [3.964(2) Å].^[13]

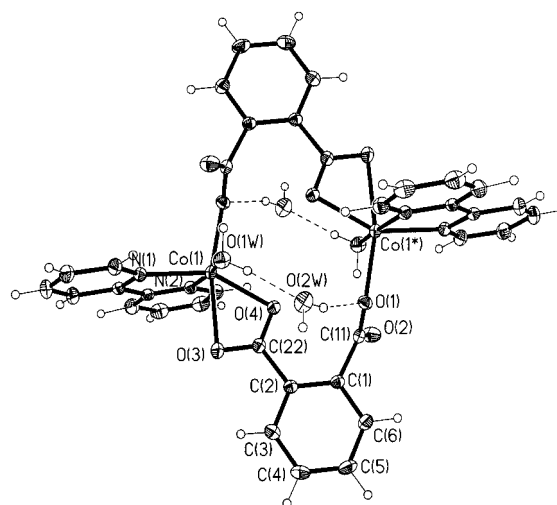


Figure 9. Discrete dinuclear molecule in compound 4.

Table 4. Selected bond lengths [Å] and angles [$^\circ$] for compounds 4 and 5.^[a]

4		5	
$\text{Co}(1)-\text{O}(1)^1$	2.076(1)	$\text{Co}(1)-\text{O}(1)^2$	2.054(6)
$\text{Co}(1)-\text{O}(3)$	2.235(2)	$\text{Co}(1)-\text{O}(3)$	2.196(5)
$\text{Co}(1)-\text{O}(4)$	2.141(1)	$\text{Co}(1)-\text{O}(4)$	2.181(5)
$\text{Co}(1)-\text{N}(1)$	2.097(1)	$\text{Co}(1)-\text{N}(1)$	2.151(7)
$\text{Co}(1)-\text{N}(2)$	2.127(1)	$\text{Co}(1)-\text{N}(2)$	2.108(6)
$\text{Co}(1)-\text{O}(1\text{w})$	2.118(1)	$\text{Co}(1)-\text{O}(1\text{w})$	2.095(5)
$\text{O}(1)^1-\text{Co}(1)-\text{O}(3)$	165.32(5)	$\text{O}(1)^2-\text{Co}(1)-\text{O}(3)$	154.8(2)
$\text{O}(1)^1-\text{Co}(1)-\text{O}(4)$	105.44(5)	$\text{O}(1)^2-\text{Co}(1)-\text{O}(4)$	96.9(2)
$\text{O}(1)^1-\text{Co}(1)-\text{N}(1)$	102.49(5)	$\text{O}(1)^2-\text{Co}(1)-\text{N}(1)$	85.2(2)
$\text{O}(1)^1-\text{Co}(1)-\text{N}(2)$	91.56(5)	$\text{O}(1)^2-\text{Co}(1)-\text{N}(2)$	117.8(2)
$\text{O}(1)^1-\text{Co}(1)-\text{O}(1\text{w})$	93.04(5)	$\text{O}(1)^2-\text{Co}(1)-\text{O}(1\text{w})$	89.3(2)
$\text{O}(3)-\text{Co}(1)-\text{O}(4)$	60.15(5)	$\text{O}(3)-\text{Co}(1)-\text{O}(4)$	60.3(2)
$\text{N}(1)-\text{Co}(1)-\text{O}(3)$	92.18(5)	$\text{N}(1)-\text{Co}(1)-\text{O}(3)$	102.7(2)
$\text{N}(1)-\text{Co}(1)-\text{O}(4)$	150.90(5)	$\text{N}(1)-\text{Co}(1)-\text{O}(4)$	86.7(2)
$\text{N}(1)-\text{Co}(1)-\text{N}(2)$	77.37(5)	$\text{N}(2)-\text{Co}(1)-\text{O}(4)$	139.0(2)
$\text{N}(1)-\text{Co}(1)-\text{O}(1\text{w})$	93.63(6)	$\text{N}(2)-\text{Co}(1)-\text{O}(3)$	87.3(2)
$\text{N}(2)-\text{Co}(1)-\text{O}(3)$	92.23(5)	$\text{N}(2)-\text{Co}(1)-\text{N}(1)$	76.0(2)
$\text{N}(2)-\text{Co}(1)-\text{O}(4)$	93.76(5)	$\text{O}(1\text{w})-\text{Co}(1)-\text{O}(4)$	111.1(2)
$\text{O}(1\text{w})-\text{Co}(1)-\text{O}(3)$	85.35(5)	$\text{O}(1\text{w})-\text{Co}(1)-\text{O}(3)$	89.5(2)
$\text{O}(1\text{w})-\text{Co}(1)-\text{O}(4)$	92.89(5)	$\text{O}(1\text{w})-\text{Co}(1)-\text{N}(1)$	161.9(2)
$\text{O}(1\text{w})-\text{Co}(1)-\text{N}(2)$	170.61(5)	$\text{O}(1\text{w})-\text{Co}(1)-\text{N}(2)$	91.4(2)

[a] Symmetry transformations used to generate equivalent atoms: ¹: $-x + 1, -y, -z + 1$; ²: $-x + 2, -y + 1, z + 1/2$.

Both the coordinated and solvate water molecules generate an extensive hydrogen-bonding network in **4**. The coordinated water molecule O(1w) is involved in intermolecular H-bonding $[O(1w) \cdots O(2) (-x + 1, -y, -z + 1) = 2.695(2) \text{ \AA}]$. A pair of identical H_2O molecules [O(2w)], one above and the other below the plane of the 14-membered cycle, which additionally constrict the dimer, form hydrogen bonds as donors with the O(1) atoms of the monocoordinated carboxylate groups $[O(2w) \cdots O(1) = 2.871(2) \text{ \AA}]$ and as acceptors with the coordinated water molecules $[O(1w) \cdots H \cdots O(2w) = 2.722(2) \text{ \AA}]$. The second donor function of the O(2w) molecule reduces the organization of layers of dimers (Figure 10) parallel to the (101) plane. These layers are held together by π - π interactions between antiparallel bpy molecules with an average deviation of the bpy atoms from the adjacent ring of $3.41(3) \text{ \AA}$.

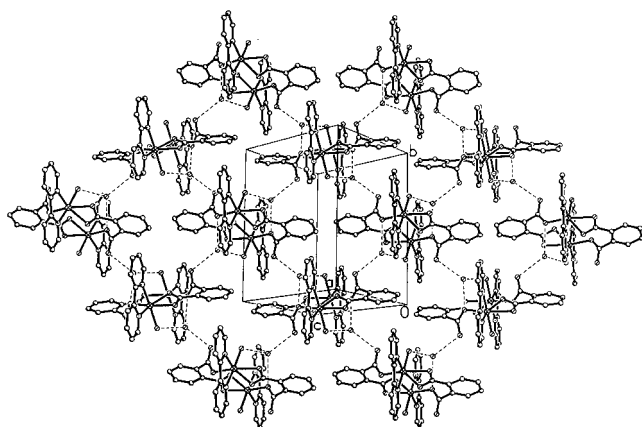


Figure 10. Packing diagram of compound **4**. Hydrogen atoms have been omitted for clarity and hydrogen bonds are indicated by dotted lines.

$[Co(Pht)(bpy)(H_2O)]_n$ (**5**)

The crystal structure of **5** consists of $[Co(Pht)(bpy)(H_2O)]$ entities (Figure 11) as in **4**, but they

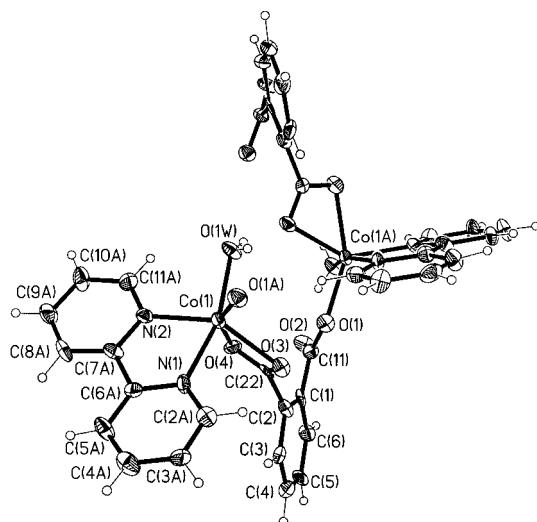


Figure 11. A fragment of the helical polymeric chain in compound **5** with the numbering scheme.

are joined into a helical polymeric chain (Figure 12). It is necessary to note that **5** is isostructural with $[Zn(Pht)(bpy)(H_2O)]_n$.^[33] The coordination polyhedron of the Co atom is composed of the same donor atoms as in **4** and is also distorted. The bond lengths range from $2.054(1)$ to $2.196(5) \text{ \AA}$ and the bond angles from $60.3(2)^\circ$ to $117.8(2)^\circ$ (Table 4). The Co–O(3) and Co–O(4) bond lengths for the bidentate carboxylate group are similar [$2.196(5)$ and $2.181(5) \text{ \AA}$], and that is a rather surprising result in light of the 1,3-chelating function of the Pht ligand.^[11,14,15] There is a principal difference in the dihedral

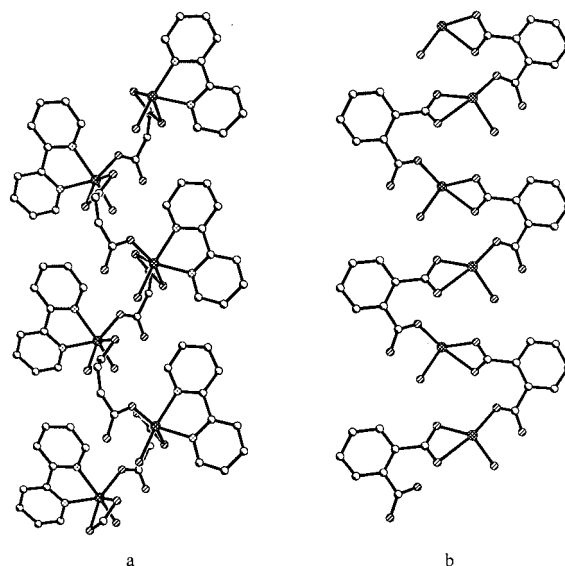


Figure 12. View along the c -axis of the single helical chain in compound **5** with bpy wings (a) and Pht wings (b).

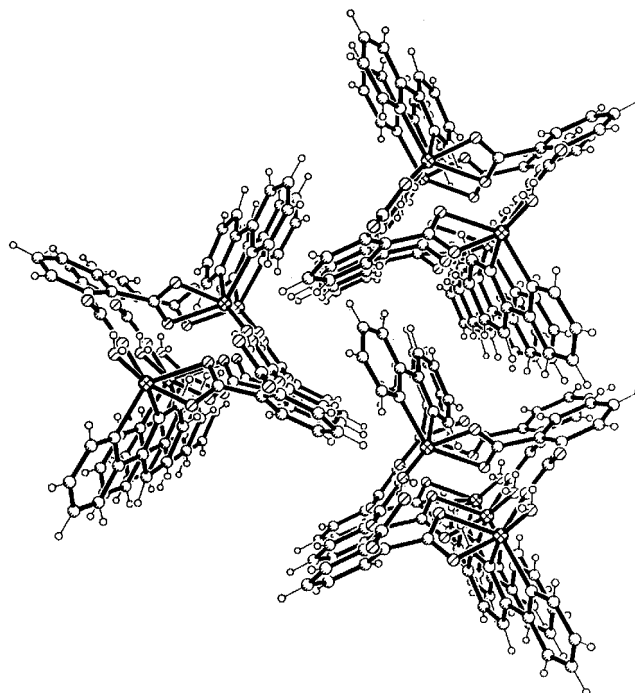


Figure 13. Crystal packing of the helical chains in compound **5**.

angles between the planes of the coordinated carboxylate group and the aromatic ring in compounds **5** and **4**. In the former, this angle is equal to 61.5° , whereas in the latter the coordinated carboxylate group lies almost in the plane of the aromatic ring (the dihedral angle is 8°). The second carboxylate group of the phthalate dianion is monocoordinated to its adjacent Co atom [$\text{Co}-\text{O}(1) = 2.054(6) \text{ \AA}$]. The tridentate chelate-bridging function of the Pht ligand leads to the organization of the infinite helical chain along the c -axis with a pitch of 8.432 \AA (Figure 12). The neighboring $\text{Co}\cdots\text{Co}$ distance is $5.546(1) \text{ \AA}$, slightly shorter than the $\text{Zn}\cdots\text{Zn}$ distance in $[\text{Zn}(\text{Pht})(\text{bpy})(\text{H}_2\text{O})]_n$ (5.633 \AA)^[33] and much shorter than that in the helix of $[\text{Co}(\text{Pht})(4\text{-MeIm})_2]_n$ [$6.247(1) \text{ \AA}$].^[15] The adjacent complexes within the chain are joined additionally through two $\text{O}-\text{H}\cdots\text{O}$ hydrogen bonds between the coordinated water molecule and carboxylate oxygen atoms $\text{O}(2)$ and $\text{O}(4)$ of $2.570(8)$ and $2.760(8) \text{ \AA}$, respectively. The chains are held together by van der Waals interactions (Figure 13).

Magnetic Studies

The temperature dependence of the molar magnetic susceptibility, χ_M , of complex **1** indicates a diamagnetic behavior. This corresponds to low-spin Co^{III} ($S = 0$) ions.

The thermal dependence of $\chi_M T$ ($\chi_M T$ being the product of the molar magnetic susceptibility and the temperature) and the simulated curve for a powdered sample of the dinuclear complex **2** are shown in Figure 14. The room-temperature $\chi_M T$ value of $6.0 \text{ emu K mol}^{-1}$ agrees well with the calculated value of $6.0 \text{ emu K mol}^{-1}$ for a high-spin Co^{II} compound ($S = 3/2$) with $g = 2.55$.^[34] The gradual decrease of $\chi_M T$ upon lowering the temperature is typical for high-spin Co^{II} . This decrease of $\chi_M T$ is mainly due to zero-field splitting. Below 100 K , a possible weak antiferromagnetic interaction between neighboring Co^{II} ions provokes a further decrease of the $\chi_M T$ values. A simulation within the temperature range $5\text{--}300 \text{ K}$ with a g -value of 2.55 , an axial zero-field splitting parameter^[34,35] of $|D| = 70 \text{ cm}^{-1}$, and an exchange parameter, J , of -0.1 cm^{-1} gives the best agreement with the experimental data.

The room-temperature $\chi_M T$ value of $3.05 \text{ emu K mol}^{-1}$ for compound **3** (Figure 15) agrees quite well with the calculated value of $3.17 \text{ emu K mol}^{-1}$ for a high-spin Co^{II} compound ($S = 3/2$) with $g = 2.6$.^[34] The gradual decrease of $\chi_M T$ upon lowering the temperature is typical for high-spin Co^{II} . This decrease of $\chi_M T$ is mainly due to zero-field splitting. A simulation within the temperature range $25\text{--}300 \text{ K}$ with the parameters $|D| = 80 \text{ cm}^{-1}$ and $g = 2.6$ reproduces the experimental data quite well. At lower temperatures, the measured susceptibility shows a steeper decrease. This is probably due to weak antiferromagnetic intermolecular interactions between the Co^{II} complexes.

The thermal dependence of $\chi_M T$ of complex **5** is depicted in Figure 16. Attempts to obtain a satisfactory simulation for this linear-chain compound of Co^{II} ions were not successful. However, only to give an impression of the deviation from a single ion behavior, a simulation^[36] within the

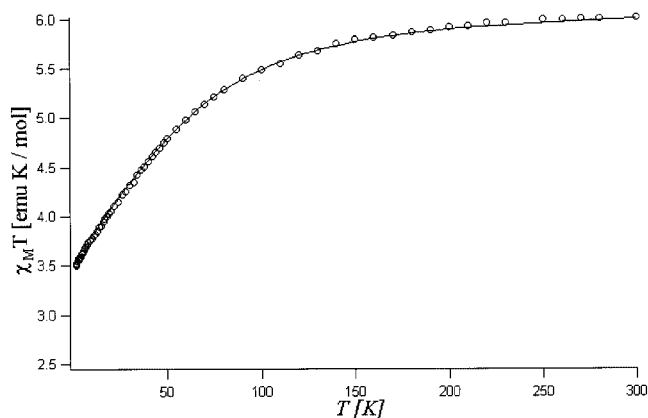


Figure 14. The circles correspond to the temperature dependence $\chi_M T$ for $[(\text{bpy})_2\text{Co}(\text{Pht})\text{H}(\text{Pht})\text{Co}(\text{bpy})_2](\text{HPht})(\text{H}_2\text{Pht})\cdot 2\text{H}_2\text{O}$ (**2**). A simulation from 5 to 300 K with the parameters^[34–36] $|D| = 70 \text{ cm}^{-1}$, $g = 2.55$, and $J = -0.1 \text{ cm}^{-1}$ is depicted as a line.

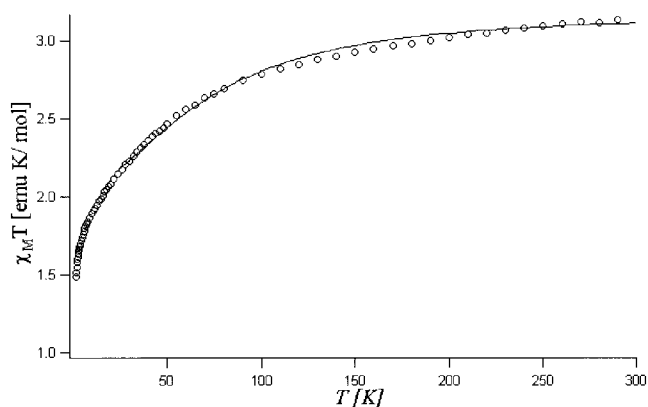


Figure 15. The temperature dependence, $\chi_M T$, for $[\text{Co}(\text{Pht})(\text{bpy})(\text{H}_2\text{O})_3]\cdot 3\text{H}_2\text{O}$ (**3**) is depicted as circles. The line corresponds to a simulation from 25 to 300 K with the parameters $|D| = 80 \text{ cm}^{-1}$ and $g = 2.6$.

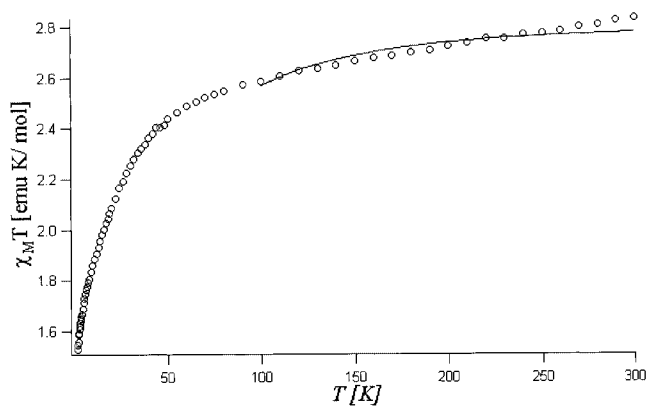


Figure 16. The temperature dependence, $\chi_M T$, for the chain complex $[\text{Co}(\text{Pht})(\text{bpy})(\text{H}_2\text{O})]_n$ (**5**) is depicted as circles. A simulation for a single-ion behavior within the temperature range of 100 to 300 K by using a typical parameter set of $|D| = 65 \text{ cm}^{-1}$ and $g = 2.45$ is shown as a line.

temperature range of 100 to 300 K , with a typical parameter set of $|D| = 65 \text{ cm}^{-1}$ and $g = 2.45$, is depicted in Figure 16. Obviously, intrachain magnetic-exchange interactions have a pronounced effect.

Conclusions

The reaction of cobalt(II) anions with *o*-phthalic acid and bidentate bipyridine ligands has produced some intriguing complexes. Complexes of different nuclearity are obtained depending on the temperature of the reaction: the mononuclear $[\text{Co}^{\text{III}}(\text{CO}_3)(\text{bpy})_2](\text{Pht}) \cdot 16\text{H}_2\text{O}$ (**1**) and $[\text{Co}(\text{Pht})(\text{bpy})(\text{H}_2\text{O})_3] \cdot 3\text{H}_2\text{O}$ (**3**) complexes, the open $[(\text{bpy})_2\text{Co}(\text{Pht})\text{H}(\text{Pht})\text{Co}(\text{bpy})_2](\text{HPht})(\text{H}_2\text{Pht}) \cdot 2\text{H}_2\text{O}$ (**2**) and cyclic dinuclear $[\text{Co}(\text{Pht})(\text{bpy})(\text{H}_2\text{O})_2]_n \cdot 2\text{H}_2\text{O}$ (**4**), and polynuclear $[\text{Co}(\text{Pht})(\text{bpy})(\text{H}_2\text{O})]_n$ (**5**). Moreover, in complex **1** the oxidation of cobalt(II) to cobalt(III) ions has occurred. The structural trends displayed in **1–5** illustrate the extraordinarily rich binding abilities of the carboxylate groups of the *o*-phthalate ligand and their ability to form extensive hydrogen-bonding interactions and build supramolecular architectures. The variable-temperature magnetic data indicate a weak antiferromagnetic interaction between neighboring Co^{II} centers in both the open dinuclear complex **2** and mononuclear complex **3**, whereas complex **1** is a rare example containing low-spin Co^{III} ($S = 0$) ions.

Experimental Section

General: All reagents were purchased from commercial sources and used as received. IR spectra were recorded with a Perkin–Elmer Spectrum One spectrometer in the region $4000\text{--}400\text{ cm}^{-1}$ using KBr pellets. TG analyses were carried out with a Mettler–Toledo TA 50 in dry dinitrogen (60 mL min^{-1}) at a heating rate of 5°C min^{-1} . Magnetic susceptibility data of powdered samples were collected with an MPMS Quantum Design SQUID magnetometer (XL-5) in the temperature range $300\text{--}1.8\text{ K}$ and at a field of 1000 G . The samples were placed in a Saran foil bag and a straw was used as the sample holder. The output data were corrected for the experimentally determined diamagnetism of the sample holder and the diamagnetism of the sample calculated from Pascal's constants. The program MAGPACK^[36] was used to model the experimental magnetic susceptibility data.

Synthesis of $[\text{Co}(\text{CO}_3)(\text{bpy})_2](\text{Pht}) \cdot 16\text{H}_2\text{O}$ (1**):** A warm solution of H_2Pht (1.66 g, 10 mmol) and bpy (1.56 g, 10 mmol) in water (20 mL) was added to a suspension of $\text{CoCO}_3 \cdot \text{Co}(\text{OH})_2 \cdot n\text{H}_2\text{O}$ (1.18 g) and K_2CO_3 (1.38 g, 10 mmol) in water (30 mL). The resulting mixture was stirred at 60°C for 30 min. The precipitated solid was removed immediately and the filtrate allowed to cool to room temp. Dark-red crystals of **1** suitable for X-ray diffraction studies were filtered off after two weeks, and washed with water, EtOH, and dried in air. Yield: 1.00 g (30.4% based on bpy). $\text{C}_{50}\text{H}_{68}\text{Co}_2\text{N}_8\text{O}_{26}$ (1315.0): calcd. C 45.67, H 5.21, N 8.52; found C 45.71, H 5.15, N 8.48. IR (KBr): $\tilde{\nu} = 3384\text{ br}, 3116\text{ m}, 3086\text{ m}, 3061\text{ m}, 3032\text{ m}, 1678\text{ vs}, 1639\text{ s}, 1606\text{ s}, 1563\text{ s}, 1501\text{ m}, 1472\text{ s}, 1449\text{ s}, 1403\text{ s}, 1382\text{ s}, 1318\text{ m}, 1282\text{ w}, 1247\text{ m}, 1202\text{ s}, 1157\text{ m}, 1123\text{ w}, 1109\text{ w}, 1075\text{ w}, 1037\text{ w}, 1025\text{ w}, 1004\text{ w}, 822\text{ m}, 773\text{ vs}, 751\text{ sh}, 729\text{ s}, 692\text{ w}, 676\text{ w}, 652\text{ m}, 509\text{ m}, 484\text{ w cm}^{-1}$.

Synthesis of $[(\text{bpy})_2\text{Co}(\text{Pht})\text{H}(\text{Pht})\text{Co}(\text{bpy})_2](\text{HPht})(\text{H}_2\text{Pht}) \cdot 2\text{H}_2\text{O}$ (2**):** H_2Pht (3.32 g, 20 mmol) and bpy (3.12 g, 20 mmol) were added to a suspension of $\text{CoCO}_3 \cdot \text{Co}(\text{OH})_2 \cdot n\text{H}_2\text{O}$ (2.3 g) in water (50 mL). The resulting mixture was stirred at 80°C for 10 min. The precipitated solid containing unreacted cobalt(II) carbonate was removed immediately and the filtrate allowed to cool to room temp. Large red crystals were filtered off after a week, washed with water, and

dried in air. Yield: 4.52 g (62.87% based on bpy). $\text{C}_{72}\text{H}_{56}\text{Co}_2\text{N}_8\text{O}_{18}$ (1439.1): calcd. C 60.09, H 3.92, N 7.79; found C 59.90, H 3.86, N 7.59. IR (KBr): $\tilde{\nu} = 3428\text{ br}, 3073\text{ m}, 3035\text{ sh}, 1717\text{ s}, 1600\text{ vs}, 1579\text{ vs}, 1564\text{ sh}, 1538\text{ s}, 1493\text{ sh}, 1475\text{ vs}, 1444\text{ vs}, 1411\text{ vs}, 1366\text{ s}, 1315\text{ m}, 1293\text{ m}, 1251\text{ m}, 1177\text{ m}, 1159\text{ m}, 1075\text{ m}, 1059\text{ m}, 1022\text{ s}, 796\text{ m}, 773\text{ vs}, 736\text{ s}, 715\text{ m}, 683\text{ w}, 650\text{ m}, 576\text{ m cm}^{-1}$. Single crystals suitable for diffraction studies were obtained by recrystallization of **2** from a hot aqueous solution.

Synthesis of $[\text{Co}(\text{Pht})(\text{bpy})(\text{H}_2\text{O})_3] \cdot 3\text{H}_2\text{O}$ (3**) and $[\text{Co}(\text{Pht})(\text{bpy})(\text{H}_2\text{O})]_n$ (**5**). Method A:** Cobalt(II) carbonate (1.18 g) was added to a hot solution of H_2Pht (1.69 g, 10 mmol) and bpy (1.56 g, 10 mmol) in water (50 mL). The resulting mixture was heated at reflux for 45 min. The precipitated solid was removed by filtration from the hot solution, and the filtrate allowed to cool to room temp. Cherry-colored crystalline **5** and large, rose-colored crystals of **3** suitable for X-ray investigation were collected by filtration after a week, washed with water and dried in air. The crystals of **3** and **5** were separated by hand. The yields of compounds **5** and **3** were 0.78 g (19.65%) and 0.3 g (12.1%), respectively. An additional batch of **3** was obtained by keeping the mother filtrate in air for 2 weeks. **3:** $\text{C}_{18}\text{H}_{24}\text{CoN}_2\text{O}_{10}$ (487.32): calcd. C 44.36, H 4.96, N 5.75; found C 44.28, H 4.68, N 5.67. IR (KBr): $\tilde{\nu} = 3230\text{ br}, 1652\text{ sh}, 1602\text{ vs}, 1568\text{ vs}, 1484\text{ s}, 1444\text{ vs}, 1404\text{ vs}, 1315\text{ m}, 1250\text{ m}, 1172\text{ m}, 1159\text{ m}, 1104\text{ w}, 1087\text{ m}, 1060\text{ m}, 1023\text{ s}, 840\text{ s}, 820\text{ s}, 764\text{ vs}, 736\text{ vs}, 701\text{ s}, 652\text{ s}, 632\text{ m cm}^{-1}$. The identity of **5** was established by comparison of IR data with the crystallographically characterized precipitate from Method B, and by elemental analysis (found for compound **5**: C 54.11, H 3.45, N 6.84). **Method B:** A solution of KHPht (2.04 g, 10 mmol) in 20 mL of water was added to a hot solution of $\text{Co}(\text{O}_2\text{CMe})_2 \cdot 4\text{H}_2\text{O}$ (2.49 g, 10 mmol) and bpy (1.56 g, 10 mmol) in 20 mL of MeOH. The resulting cherry-colored solution was stirred and heated for 1 h. Crystals of compound **5** suitable for X-ray diffraction studies crystallized after several days, and they were then filtered off, washed with MeOH, and dried in air. Yield: 3.00 g (75.6%). $\text{C}_{18}\text{H}_{14}\text{CoN}_2\text{O}_5$ (397.24): calcd. C 54.43, H 3.55, N 7.05, Co 14.84; found C 54.43, H 3.61, N 6.99, Co 14.80. IR (KBr): $\tilde{\nu} = 3274\text{ br}, 3119\text{ m}, 3078\text{ m}, 1610\text{ s}, 1600\text{ s}, 1578\text{ s}, 1542\text{ vs}, 1492\text{ s}, 1474\text{ s}, 1446\text{ vs}, 1420\text{ vs}, 1384\text{ s}, 1314\text{ m}, 1262\text{ w}, 1252\text{ m}, 1175\text{ m}, 1152\text{ m}, 1085\text{ m}, 1057\text{ m}, 1041\text{ w}, 973\text{ w}, 921\text{ w}, 869\text{ m}, 824\text{ m}, 815\text{ m}, 763\text{ vs}, 737\text{ s}, 721\text{ m}, 692\text{ s}, 651\text{ s}, 631\text{ m}, 576\text{ w}, 456\text{ m cm}^{-1}$. **Method C:** $\text{Co}(\text{O}_2\text{CMe})_2 \cdot 4\text{H}_2\text{O}$ (0.25 g, 1 mmol) in 10 mL of MeOH was added to a hot solution of H_2Pht (0.17 g, 1 mmol) and bpy (0.16 g, 1 mmol) in 15 mL of MeOH. The resulting cherry-colored solution was heated at reflux for 1 h. Water (1 mL) was then added to the solution and it was allowed to slowly evaporate at room temp. over 3 weeks to give a crystalline precipitate of **5** and several crystals of **4** suitable for diffraction studies. The yield of **5** was 0.25 g (62.5%). It was further identified by comparison of its IR spectrum with the crystallographically characterized precipitate from Method B, and by elemental analysis; found for the title compound **5**: C 54.30, H 3.48, Co 14.90, N 7.01.

X-ray Crystallographic Study: Experimental data for **2a** were collected with an Enraf–Nonius CAD4 single-crystal diffractometer with $\text{Cu-K}\alpha$ radiation at 140 K and were processed using a locally written program.^[37] Experimental data for all other crystals were obtained with a KUMA KM4CCD- κ -axis diffractometer with graphite-monochromated $\text{Mo-K}\alpha$ radiation at 130 K for **1**, 293 K for **2b** and **4**, 130 K for **3**, and at 170 K for **5**. The data were processed using the KUMA diffraction (Wrocław, Poland) program. Crystal data and details of data collection and refinement for **1–5** are given in Table 5. The structures were solved by direct methods (SHELXS-97)^[38] and refined by the full-matrix least-squares method on F^2 (SHELXL-97)^[39] with an anisotropic approach for

Table 5. Crystal data and structure refinements of compounds **1–5**.

	1	2a	2b	3	4	5
Empirical formula	C ₅₀ H ₆₈ Co ₂ N ₈ O ₂₆	C ₇₂ H ₅₆ Co ₂ N ₈ O ₁₈	C ₇₂ H ₅₆ Co ₂ N ₈ O ₁₈	C ₁₈ H ₂₄ CoN ₂ O ₁₀	C ₁₈ H ₁₆ CoN ₂ O ₆	C ₁₈ H ₁₄ CoN ₂ O ₅
Formula mass	1314.98	1439.10	1439.11	487.32	415.26	397.24
Temperature [K]	130(2)	140(2)	293(2)	130(2)	293(2)	170(2)
Wavelength [Å]	0.71073	1.54178	0.71073	0.71073	0.71073	0.71073
Crystal size [mm]	0.7 × 0.7 × 0.3	0.3 × 0.4 × 0.3	0.6 × 0.6 × 0.3	0.8 × 0.4 × 0.4	0.5 × 0.5 × 0.3	0.25 × 0.1 × 0.05
Crystal system	monoclinic	triclinic	triclinic	monoclinic	monoclinic	orthorhombic
Space group	<i>P</i> 2 ₁ / <i>c</i>	<i>P</i> $\bar{1}$	<i>P</i> $\bar{1}$	<i>P</i> 2 ₁ / <i>c</i>	<i>P</i> 2 ₁ / <i>n</i>	<i>Pna</i> 2 ₁
<i>a</i> [Å]	14.046(3)	10.901(2)	15.324(3)	8.959(2)	11.520(2)	10.077(2)
<i>b</i> [Å]	14.693(3)	11.690(2)	20.702(4)	18.711(4)	13.072(3)	19.098(4)
<i>c</i> [Å]	28.904(6)	14.022(3)	31.835(6)	12.757(3)	11.957(2)	8.432(2)
α [°]	90.	111.16(3)	104.79(3)	90	90	90
β [°]	91.94(3)	105.79(3)	93.45(3)	102.57(3)	107.25(3)	90
γ [°]	90	91.40(3)	92.95(3)	90.	90	90
<i>Z</i> , <i>D</i> _c [g cm ⁻³]	4, 1.465	1, 1.504	6, 1.475	4, 1.551	4, 1.604	4, 1.626
μ [mm ⁻¹]	0.647	4.795	0.594	0.881	1.038	1.091
<i>F</i> (000)	2744	742	4452	1012	852	812
θ range for data coll. [°]	3.41–25.03	3.54–69.98	3.40–25.03	3.45–29.82	3.57–26.37	3.79–25.02
Limiting indices	–16 ≤ <i>h</i> ≤ 16 –17 ≤ <i>k</i> ≤ 13 –34 ≤ <i>l</i> ≤ 34	0 ≤ <i>h</i> ≤ 13 –14 ≤ <i>k</i> ≤ 14 –17 ≤ <i>l</i> ≤ 16	–9 ≤ <i>h</i> ≤ 18 –24 ≤ <i>k</i> ≤ 24 –37 ≤ <i>l</i> ≤ 37	–12 ≤ <i>h</i> ≤ 12 –16 ≤ <i>k</i> ≤ 25 –17 ≤ <i>l</i> ≤ 16	–11 ≤ <i>h</i> ≤ 14 –16 ≤ <i>k</i> ≤ 16 –14 ≤ <i>l</i> ≤ 14	–11 ≤ <i>h</i> ≤ 5 –20 ≤ <i>k</i> ≤ 22 –10 ≤ <i>l</i> ≤ 6
Reflections collected/unique	61380/10503	5951/5951	83789/33922	23547/5496	9325/3507	4658/2064
Completeness to θ_{\max}	[<i>R</i> (int) = 0.0552] 99.6%	[<i>R</i> (int) = 0] 99.0%	[<i>R</i> (int) = 0.0389] 98.7%	[<i>R</i> (int) = 0.0395] 91.8%	[<i>R</i> (int) = 0.0189] 99.6%	[<i>R</i> (int) = 0.0704] 98.8%
Data/restraints/parameters	10503/52/903	5951/6/481	33922/8/2771	5496/0/376	3507/0/309	2064/1/236
Goodness-of-fit on <i>F</i> ²	1.021	1.023	1.116	1.079	1.058	1.033
Final <i>R</i> indices [<i>I</i> > 2σ(<i>I</i>)]	<i>R</i> ₁ = 0.0491, <i>wR</i> ₂ = 0.1389	<i>R</i> ₁ = 0.0401, <i>wR</i> ₂ = 0.1058	<i>R</i> ₁ = 0.0644, <i>wR</i> ₂ = 0.1956	<i>R</i> ₁ = 0.0346, <i>wR</i> ₂ = 0.0831	<i>R</i> ₁ = 0.0271, <i>wR</i> ₂ = 0.0690	<i>R</i> ₁ = 0.0568, <i>wR</i> ₂ = 0.1089
<i>R</i> indices (all data)	<i>R</i> ₁ = 0.0599, <i>wR</i> ₂ = 0.1488	<i>R</i> ₁ = 0.0489, <i>wR</i> ₂ = 0.1102	<i>R</i> ₁ = 0.1250, <i>wR</i> ₂ = 0.2312	<i>R</i> ₁ = 0.0384, <i>wR</i> ₂ = 0.0858	<i>R</i> ₁ = 0.0301, <i>wR</i> ₂ = 0.0714	<i>R</i> ₁ = 0.0770, <i>wR</i> ₂ = 0.1183
Largest diff. peak/hole [e Å ⁻³]	0.821/–0.667	0.349/–0.661	0.465/–0.836	0.558/–0.695	0.276/–0.270	0.459/–0.473

the non-hydrogen atoms for **1**, **2a**, **3**, **4**, and **5**. The crystals of **2b** have a substructure: I_{exp} for *hkl* reflections with $l = 2n \gg I_{\text{exp}}$ for *hkl* with $l = 2n + 1$. The structure of **2b** was refined by using the Konnert–Hendrickson conjugate-gradient algorithm (CGLS) at the early stages, and then the blocked full-matrix refinement was performed. Hydrogen atoms were located from the difference syntheses of electronic density, except for H of disordered phthalate moieties and water molecules. Localized hydrogen atoms were included in the subsequent refinement in the riding-model approximation for **1**, **2a**, **2b**, and **5**. For **3** and **4**, H-atoms were refined in an isotropic approximation. CCDC-258617 (**1**), -258618 (**2a**), -258619 (**2b**), -258939 (**3**), -258620 (**4**), and -258621 (**5**) contain the supplementary crystallographic data for this paper. These data can be obtained free of charge from The Cambridge Crystallographic Data Center via www.ccdc.cam.ac.uk/data_request/cif.

Supporting Information (see footnote on the first page of this article): Figure S1 shows the correlation between the two unit cells of **2a** and **2b**. Hydrogen-bonding interactions in compound **1** (Table S1) and compound **3** (Table S2).

Acknowledgments

This work was supported by the Swiss National Science Foundation (SCOPES 7MDPJ065712.01/1). The authors gratefully acknowledge the assistance of Professor Bocelli, Centro di Studio per la Strutturistica Diffattometrica del CNR, Parma, Italy, in the collection of crystallographic data sets for compound **2b**.

- a) R. C. Mehrotra, R. Bohra, *Metal Carboxylates*, Academic Press, New York, **1983**; b) C. N. R. Rao, S. Natarajan, R. Vaidhyanathan, *Angew. Chem. Int. Ed.* **2004**, *43*, 1466–1496 and references cited therein.
- a) *Catalysis in Organic Synthesis* (Ed.: W. H. Jones), Academic Press, New York, **1980**; b) R. A. Sheldon, J. K. Kochi, *Metal Catalyzed Oxidations of Organic Compounds*, Academic Press, New York, **1981**; c) V. V. Goncharuk, G. L. Kamalov, G. A. Kovtun, E. S. Rudakov, V. K. Yatsimirsky *Catalysis. Mechanisms of Homogeneous and Heterogeneous Catalysis, Cluster Approaches*, Naukova Dumka, Kiev, **2002**, p. 541 (in Russian); d) T. Szymanska-Buzar, J. J. Ziolkowski, *Koord. Khim.* **1976**, *2*, 1172–1191 (in Russian); *Chem. Abstr.* **1977**, *86*, 79306m. e) T. Szymanska-Buzar, J. J. Ziolkowski, *J. Mol. Catal.* **1981**, *11*, 371–381; f) S. Uemura, S. R. Patil, *Chem. Lett.* **1982**, *11*, 1743–1746; g) G. Rousselet, C. Chassagnard, P. Capdevielle, M. Maumy, *Tetrahedron Lett.* **1996**, *37*, 8497–8500; h) U. Schuchardt, M. C. Guerreiro, G. B. Shul'pin, *Russ. Chem. Bull.* **1998**, *107*, 247–252; i) E. D. Park, Y.-S. Hwang, J. S. Lee, *Catal. Commun.* **2001**, *2*, 187–190; j) G. Blay, I. Fernandez, T. Gimenez, J. R. Pedro, R. Ruiz, E. Pardo, F. Lloret, M. C. Munoz, *Chem. Commun.* **2001**, 2102–2103; k) G. Suss-Fink, L. G. Cuervo, B. Therrien, H. Stoeckli-Evans, G. B. Shul'pin, *Inorg. Chim. Acta* **2004**, *357*, 475–484; l) P.-G. Lassahn, V. Lozan, G. A. Timco, P. Christian, C. Janiak, R. E. P. Winpenny, *J. Catal.* **2004**, *222*, 260–267.
- S. G. Baca, I. G. Filippova, O. A. Gherco, M. Gdaniec, Yu. A. Simonov, N. V. Gerbeleu, P. Franz, R. Basler, S. Decurtins, *Inorg. Chim. Acta* **2004**, *357*, 3419–3429.
- R. C. Squire, S. M. J. Aubin, K. Folting, W. E. Streib, D. N. Hendrickson, G. Christou, *Angew. Chem. Int. Ed. Engl.* **1995**, *34*, 887–889.

- [5] R. C. Squire, S. M. J. Aubin, K. Folting, W. E. Streib, G. Christou, D. N. Hendrickson, *Inorg. Chem.* **1995**, *34*, 6463–6471.
- [6] E. K. Brechin, R. O. Gould, S. G. Harris, S. Parsons, R. E. P. Winpenny, *J. Am. Chem. Soc.* **1996**, *118*, 11293–11294.
- [7] E. K. Brechin, S. G. Harris, S. Parsons, R. E. P. Winpenny, *Chem. Commun.* **1996**, 1439–1440.
- [8] E. K. Brechin, A. Graham, A. Parkin, S. Parson, A. M. Seddon, R. E. P. Winpenny, *J. Chem. Soc., Dalton Trans.* **2000**, 3242–3252.
- [9] C. Cañada-Vilalta, M. Pink, G. Christou, *Dalton Trans.* **2003**, 1121–1125.
- [10] N. V. Gerbelev, Yu. A. Simonov, G. A. Timco, P. N. Bourosh, J. Lipkowski, S. G. Baca, D. I. Saburov, M. D. Mazus, *Russ. J. Inorg. Chem.* **1999**, *44*, 1191–1204.
- [11] S. G. Baca, Yu. A. Simonov, N. V. Gerbelev, M. Gdaniec, P. N. Bourosh, G. A. Timco, *Polyhedron* **2001**, *20*, 831–837.
- [12] Yu. A. Simonov, M. Gdaniec, I. G. Filippova, S. G. Baca, G. A. Timco, N. V. Gerbelev, *Russ. J. Coord. Chem.* **2001**, *27*, 353–359.
- [13] S. G. Baca, I. G. Filippova, N. V. Gerbelev, Yu. A. Simonov, M. Gdaniec, G. A. Timco, O. A. Gherco, Yu. L. Malaestean, *Inorg. Chim. Acta* **2003**, *344*, 109–116.
- [14] S. G. Baca, Yu. A. Simonov, M. Gdaniec, N. V. Gerbelev, I. G. Filippova, G. A. Timco, *Inorg. Chem. Commun.* **2003**, *6*, 685–689.
- [15] S. G. Baca, S. T. Malinovskii, P. Franz, Ch. Ambrus, H. Stoeckli-Evans, N. Gerbelev, S. Decurtins, *J. Solid State Chem.* **2004**, *177*, 2841–2849.
- [16] Yu. A. Simonov, S. G. Baca, I. G. Filippova, M. Gdaniec, O. A. Gherco, N. V. Gerbelev, *Russ. J. Coord. Chem.* **2004**, *30*, 727–732.
- [17] P. Lightfoot, A. Snedden, *J. Chem. Soc., Dalton Trans.* **1999**, 3549–3551.
- [18] S.-L. Ma, D.-Z. Liao, Z.-H. Jiang, S.-P. Yan, F.-C. Xue, G.-L. Wang, *Synth. React. Inorg. Met.-Org. Chem.* **1994**, *24*, 137–146.
- [19] a) D. Poletti, D. R. Stojakovic, B. V. Prelesnik, Lj. Manojlovic-Muir, *Acta Crystallogr.* **1990**, *46*, 399–402; b) D. Poletti, D. R. Stojakovic, *Thermochim. Acta* **1992**, *205*, 225–233.
- [20] E. C. Niederhoffer, A. E. Martell, P. Rudolf, A. Clearfield, *Inorg. Chem.* **1982**, *21*, 3734–3741.
- [21] J. E. Arenas, J. I. Marcos, *Spectrochim. Acta* **1980**, *36*, 1075–1081.
- [22] G. B. Deacon, R. J. Phillips, *Coord. Chem. Rev.* **1980**, *33*, 227–250.
- [23] D. M. Palade, E. S. Il'ina, G. V. Chudaeva, *Zh. Neorg. Khim.* **1972**, *17*, 2480–2485; *Chem. Abstr.* **1973**, *78*, 51908v.
- [24] J. Kitchen, J. L. Bear, *Thermochim. Acta* **1970**, *1*, 537–544.
- [25] J. Sun, L. Yuan, K. Zhang, D. Wang, *Thermochim. Acta* **2000**, *343*, 105–109.
- [26] E. M. Abd Alla, M. I. Abdel-Hamid, *J. Therm. Anal. Calorim.* **2000**, *62*, 769–780.
- [27] K. Das, U. C. Sinha, C. Chatterjee, A. Mishnev, *Z. Kristallogr.* **1993**, *205*, 316–318.
- [28] E. D. McKenzie, *J. Chem. Soc. A* **1969**, 1655–1667.
- [29] Ch. Janiak, *J. Chem. Soc., Dalton Trans.* **2000**, 3885–3896.
- [30] D. Braga, A. Angeloni, L. Maini, A. W. Gotz, F. Grepioni, *New J. Chem.* **1999**, *23*, 17–24.
- [31] D. Poletti, L. Karanovic, B. V. Prelesnik, *Acta Crystallogr., Sect. C* **1990**, *46*, 2465–2467.
- [32] S. G. Baca, I. G. Filippova, P. Franz, Ch. Ambrus, M. Gdaniec, H. Stoeckli-Evans, Yu. A. Simonov, O. A. Gherco, T. Bejan, N. Gerbelev, S. Decurtins, *Inorg. Chim. Acta* **2005**, *358*, 1762–1770.
- [33] J.-C. Yao, W. Huang, B. Li, S. Gou, Y. Xu, *Inorg. Chem. Commun.* **2002**, *5*, 711–714.
- [34] S. M. Ostrovsky, R. Werner, D. A. Brown, W. Haase, *Chem. Phys. Lett.* **2002**, *353*, 290–294.
- [35] O. Kahn, *Molecular Magnetism*, Wiley-VCH, New York, **1993**, p. 42.
- [36] J. J. Borrás-Almenar, J. M. Clemente-Juan, E. Coronado, B. S. Tsukerblatt, *Inorg. Chem.* **1999**, *38*, 6081–6088.
- [37] D. Belletti, *A new hardware and software system for Controlling an Enraf Nonius CAD4 single crystal diffractometer*; Centro di Studio per la Strutturistica Diffraattometrica del CNR, Parma, Italy; Interna Report 1-97, **1997**.
- [38] G. M. Sheldrick, *SHELXS-97*, Universität Göttingen, Germany, **1997**.
- [39] G. M. Sheldrick, *SHELXL-97*, Universität Göttingen, Germany, **1997**.

Received: January 5, 2005
Published Online: June 22, 2005